photonics

MDPI

Communication

Microwave Photonic Signal Generation in an Optically Injected Discrete Mode Semiconductor Laser

Da Chang [1], Zhuqiang Zhong [1], Angel Valle [2], Wei Jin [1], Shan Jiang [1], Jianming Tang [1] and Yanhua Hong [1,*]

[1] School of Computer Science and Electronic Engineering, Bangor University, Bangor LL57 1UT, UK; dkc19tns@bangor.ac.uk (D.C.); z.zhong@bangor.ac.uk (Z.Z.); w.jin@bangor.ac.uk (W.J.); s.jiang@bangor.ac.uk (S.J.); j.tang@bangor.ac.uk (J.T.)

[2] Instituto de Física de Cantabria (IFCA), Universidad de Cantabria-CSIC, E39005 Santander, Spain; valle@ifca.unican.es

* Correspondence: y.hong@bangor.ac.uk

Abstract: In this paper, microwave photonic signal generation based on the period-one dynamic of optically injected discrete mode (DM) semiconductor lasers has been experimentally demonstrated and numerically simulated. The results show that the frequency of the generated microwave increases linearly with the frequency detuning or optical injection ratio. In addition, a single optical feedback loop is sufficient to reduce the microwave linewidth without significantly deteriorating side mode suppression. The simulation results using a model considering the nonlinear dependencies of the carrier recombination agree well with the experimental results, which indicates that the nonlinear carrier recombination effect is important in determining the nonlinear dynamics of optically injected DM lasers.

Keywords: microwave photonics signal generation; discrete mode semiconductor laser; optical injection

Citation: Chang, D.; Zhong, Z.; Valle, A.; Jin, W.; Jiang, S.; Tang, J.; Hong, Y. Microwave Photonic Signal Generation in an Optically Injected Discrete Mode Semiconductor Laser. *Photonics* **2022**, *9*, 171. https://doi.org/10.3390/photonics9030171

Received: 14 February 2022
Accepted: 7 March 2022
Published: 10 March 2022

1. Introduction

In the fast-developing information society, radio and microwave signals play significant roles in the field of communication, radar, and sensing systems [1–3]. To implement high-speed transmission in wireless networks as well as high-resolution detection in radar and sensing systems, high-frequency microwave signals with salient features such as ultralow phase noise and broad tunable range are highly required. However, it is complicated and costly to generate such desired high-frequency microwaves by multiple frequency doubling based on conventional electronic circuits [4]. Moreover, such high-frequency electrical microwave signals inevitably suffer enormous attenuation in coaxial cable transmissions for most practical scenarios [5]. To address these technical challenges, the photonic approach, well known as microwave photonics, has been applied to overcome the bottleneck of microwave generation in the electrical domain. Generally speaking, photonic generation of microwave signals has superior advantages in terms of high frequency (up to millimeter-wave band), broad frequency tunability, low propagation loss in optical fibers, and high robustness to electromagnetic interference [6–36]. Additionally, recently reported InP- and silicon-based photonic integrated devices/circuits [6–8] further expand the perspective of photonic high-frequency microwave, and thus it becomes a very hot research topic in the fields of radio-over-fiber (RoF), optical signal processing, true time delay beamforming, subnoise detection, etc. [9–12].

Compared with microwave synthesis using electronics, which has been extensively explored and developed over the past decades, high-frequency microwave photonic (MWP) signal generation in the optical domain is more convenient and cost-effective. Various approaches of MWP signal generation can generally be classified into optical heterodyning [13,14], direct and external modulation [15–17], self-pulsating and mode-locking [18,19], optoelectronic oscillators (OEOs) [20–24], and laser dynamics of period-one (P1) [25–36].

The optical heterodyne technique can easily achieve terahertz photonic microwaves by beating between two optical beams with certain wavelength spacing, as such the technique has very wide tunability [13]. However, the inevitable mismatch of optical phases and fluctuated amplitudes between two noncoherent lasers results in extremely poor microwave stability, which becomes an Achilles' heel for applications requiring high stability. Direct and external modulation schemes are also very important for high-frequency MWP signal generation. The former possesses the simplest architecture for MWP signal generation, but its modulation bandwidth is limited by the relaxation oscillation frequency of the lasers, which is usually less than 15 GHz, and the modulation depth is also relatively low [15]. On the other hand, MWP signal generation utilizing external modulation can attain very high frequency and low phase noise microwave signals, but there is a drawback resulting from the insertion loss of the modulators [16]. An OEO is another paradigmatic method to obtain narrow-linewidth microwave signals in both the electrical and optical domains by introducing a feedback loop as a high-quality-factor optoelectronic oscillating cavity to a pump laser [20–24]. Consequently, the phase noise of generated microwaves can be comparable with that produced by mode-locked lasers [19], but the frequency tunability is compromised.

Recently, a competitive approach of MWP signal generation based on the P1 dynamic of semiconductor lasers has been proposed and explored [25–36]. The P1 dynamic of semiconductor lasers can be achieved by optical injection under certain injection parameters, which causes the optical output intensity of semiconductor lasers to undergo self-sustained oscillation at a microwave frequency [25]. The MWP signal is generated when the optical output of semiconductor lasers at P1 dynamic is detected by a photodetector. Due to the injection pulling effect and the redshift effect, the generated photonic microwave frequency can be tens of times higher than the relaxation resonance frequency of the semiconductor laser while a relatively simple system setup still remains to support flexible tunability [26]. Therefore, considering the characteristics such as cost, power effectiveness, and all-optical broad frequency tunability, MWP signal generation based on P1 dynamic of semiconductor lasers becomes a promising method, and it has been widely studied for different types of semiconductor lasers. For distributed feedback (DFB) semiconductor lasers, Chan et al. comprehensively studied the P1-dynamic-based photonic microwave generation, transmission, and processing, as well as its single sideband (SSB) characteristics [27–29]. Wang et al. reported continuous tunable photonic microwave generation in quantum dot semiconductor lasers [30]. For vertical-cavity surface-emitting lasers (VCSELs), Perez et al. achieved more than 20 GHz MWP signal using a single-mode VCSEL [31]. Lin et al. experimentally demonstrated microwave generation in multi-transverse-mode VCSELs by dual-beam orthogonal optical injection [32]. Li et al. numerically investigated the effect of birefringence-induced oscillation on the photonic microwave in spin VCSELs [33]. We experimentally and theoretically studied broad tunable photonic microwaves in optically injected VCSELs and discussed the suppression of second harmonic distortion [34–36]. Furthermore, to improve the quality of P1-dynamic-based photonic microwave, extensive research efforts have also been made, which mainly include extra RF source enabled subharmonic locking and stabilization [37] and optical self-locking methods, such as optoelectronic feedback [38] and single and double external cavity optical feedback [27].

As a special type of Fabry–Perot semiconductor lasers, discrete mode (DM) lasers have similar geometry structures to standard Fabry–Perot lasers but contain a small number of etching features along the ridge waveguide. This unique feature guarantees that DM lasers can achieve single longitudinal mode operation with high sidemode suppression [39]. DM lasers also have many other impressive characteristics, such as very narrow linewidth, wide temperature operation range, low cost, and easy integration [40]. These salient features undoubtedly imply that DM lasers are a good candidate for P1-dynamic-based low-phase-noise photonic microwave generation. However, the previous reports on DM lasers [41,42] do not address the photonic microwave generation in optically injected DM lasers. Therefore, in this paper, we focus on photonic microwave generation based on the

period-one dynamic of optically injected DM semiconductor lasers. The main parameters affecting the fundamental frequency, power, linewidth, and phase noise of the generated photonic microwave have been experimentally studied. In addition, optical feedback is also adopted to further optimize the linewidth of the generated microwave. Finally, a modified rate equation model is proposed to numerically analyze the frequency of the generated microwave in DM lasers.

2. Experimental Setup

The schematic diagram of the experimental setup in a slave–master laser configuration is illustrated in Figure 1. In this experiment, a commercially available TO-56 can-packaged fiber pigtailed DM laser (Eblana Photonics, Dublin, Ireland, EP1550-DM-01-FA) with a lasing wavelength of about 1550 nm is used as a slave laser (SL). The DM laser is driven by an ultralow-noise current source (YOKOGAWA, Tokyo, Japan, GS200) and the temperature is stabilized at 24 °C by a temperature controller (Tektronix, Beaverton, OR, USA, TED 200) with an accuracy of 0.01 °C. A tunable laser (Agilent, Santa Clara, CA, USA, 8164A) is used as a master laser (ML). The emission of the ML is injected into the SL after traveling through a polarization controller (PC1), a 50:50 fiber coupler (FC1), and an optical circulator (OC). The PC1 is used to match the polarization of the injection beam to the SL's polarization. The output of the DM laser passes through the OC and is divided into a feedback path and a detection path by a 90:10 fiber coupler (FC2). The feedback loop is composed of a PC2, a variable attenuator (VA), and FC1. The polarization of the feedback light is controlled by the PC2 to be parallel to the polarization of the DM laser. The detection path is further split by the FC3, and the light beams are detected by a photodetector (PD, Thorlabs, Newton, MA, USA, RXM40AF, 40 GHz bandwidth) and a high-resolution optical spectrum analyzer (OSA, APEX Technologies, Marcoussis, France, APEX 2070, 4 pm resolution), respectively. The output of the PD is recorded by an electrical spectrum analyzer (ESA, Anritsu, Atsugi, Japan, MS2667C, 30 GHz bandwidth) or an oscilloscope (OSC, Tektronix 71254C, 12.5 GHz bandwidth).

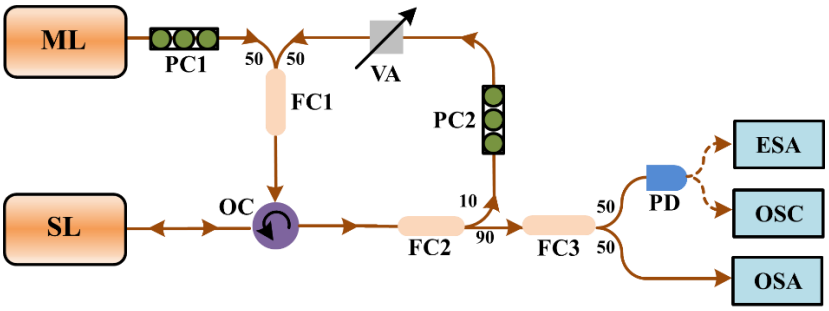

Figure 1. Schematic of the experimental setup. ML: master laser, SL: slave laser, PC: polarization control, FC: fiber coupler, OC: optical circulator, VA: variable attenuator, PD: photodetector, ESA: electrical spectrum analyzer, OSA: optical spectrum analyzer, OSC: oscilloscope.

The DM laser is biased at 30 mA, which is 2.5 times its threshold current. Under this operation condition, the output power of the free-running DM laser is 0.6 mW, and the relaxation oscillation frequency is about 6.2 GHz. In this paper, the optical injection ratio (ξ_{inj}) is defined as the optical injection power divided by the output power of the free-running DM laser, and the injection power is measured just before the injection beam enters the SL. The feedback ratio is defined as the ratio between the feedback power and the free-running DM laser output power. The feedback power is measured just before the feedback beam is fed into the DM laser. The frequency detuning (Δf) is defined as $f_{inj} - f_{SL}$, where f_{inj} and f_{SL} are the frequencies of the ML and the free-running SL, respectively. ξ_{inj} and Δf can be tuned by adjusting the output power and the frequency of the ML, respectively, and the feedback ratio is controlled by tuning the VA.

3. Experimental Results

First, the dynamical evolution of the DM laser subject to optical injection is examined. The DM laser subject to optical injection without applying optical feedback is achieved by disconnecting PC2 from the rest of the experimental setup. Figure 2 displays the (a) time series, (b) power spectra, (c) optical spectra, and (d) phase portraits, of dynamical behaviors of the DM laser with different ξ_{inj} when Δf is fixed at 10 GHz. The phase portrait is defined as the local N-th intensity as a function of $(N-1)$-th intensity. When ξ_{inj} = 0.06 (row 1), obviously, the DM laser experiences Hopf bifurcation and oscillates at P1 state with a fundamental frequency (f_0) of 10.1 GHz. The tunability and quality of microwave generated in the optically injected DM laser based on P1 dynamic will be discussed in the next section. When ξ_{inj} is increased to 0.36 (row 2), the DM laser shows period-two (P2) oscillation. After further increasing ξ_{inj} to 0.56 (row 3), the laser is in chaos dynamic. The above results indicate that the optically injected DM laser enters chaos through period doubling.

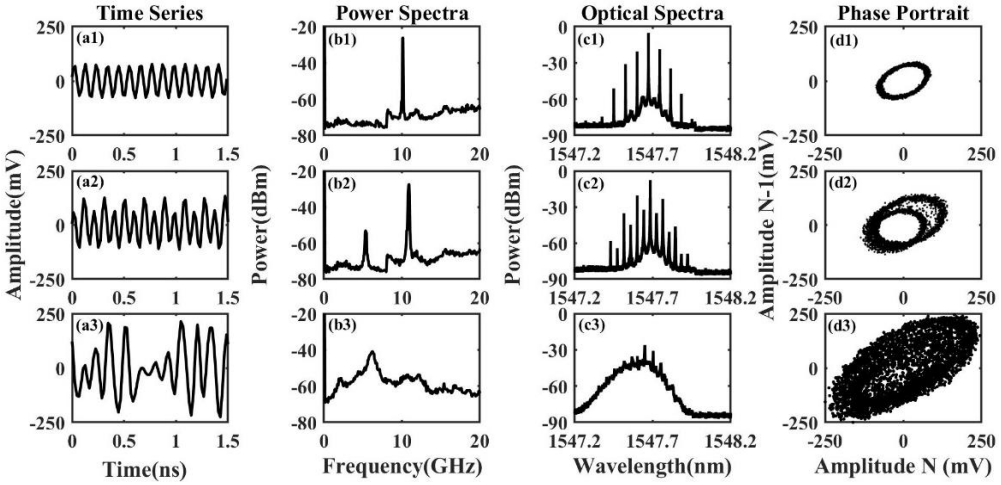

Figure 2. (**a**) Time series, (**b**) power spectra, (**c**) optical spectra, and (**d**) phase portraits of the DM laser output when Δf is 10 GHz and ξ_{inj} is 0.06 (row 1), 0.36 (row 2), and 0.56 (row 3).

In order to find P1 operation regions, the dynamics of the optically injected DM laser in a parameter space of frequency detuning Δf and injection ratio ξ_{inj} are measured and plotted in Figure 3. In the map, the stable (S), P1, P2, quasiperiod (QP), and chaos (C) dynamics are denoted by dark blue, light blue, green, orange, and red, respectively. Two non-P1 regions over the injection parameter space of 4 GHz < Δf < 14 GHz and 0.2 < ξ_{inj} < 1 and −16 GHz < Δf < −8 GHz and 0.1 < ξ_{inj} < 1 are larger than those in DFB lasers [28], but P1 dynamic still dominates on the region above the Hopf bifurcation line.

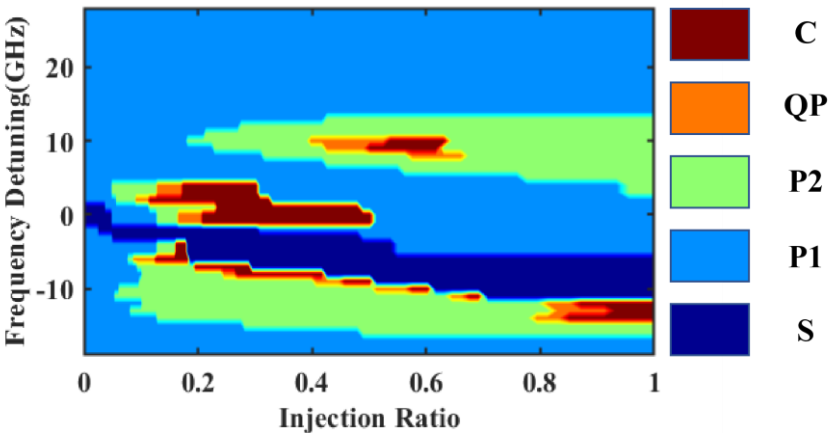

Figure 3. Dynamical map of the optically injected DM laser.

Now, we focus on MWP signal generation based on P1 dynamic in the optically injected DM laser. The effects of Δf and ξ_{inj} on the fundamental frequency (f_0) and the power of the generated microwave are presented in Figure 4. The power of the generated microwave is defined as the peak power at the fundamental frequency. Figure 4a shows the frequency of the generated microwave as a function of the injection ratio. Three frequency detunings of 15, 17, and 20 GHz are studied here because the optically injected DM laser operates at P1 dynamic over a much wider injection ratio range with $\Delta f \geq 15$ GHz. The results reveal that the microwave frequency increases linearly with the increase in injection ratio, and the change rate of the microwave frequency drops when the frequency detuning increases, which is similar to that in the DFB laser and VCSEL [28,34]. The relationship between the generated microwave power and the injection ratio is shown in Figure 4b, which shows that the power of the generated microwave first increases as the injection ratio increases, and when ξ_{inj} = 0.92, the microwave powers reach their maximum values. Upon a further increase in the injection ratio, the microwave powers decrease again. The reason for the maximum power at the injection ratio of 0.92 is that the gain distribution of the semiconductor laser is affected by the optical injection, which causes the amplitudes of the redshifted cavity resonance component and the regenerated injection component in the optical spectrum of P1 dynamic to change with the injection ratio. When the injection ratio is about 0.92, the amplitudes of the redshifted cavity resonance component and the regenerative injection component are almost the same; therefore, the microwave power reaches its maximum [28,43]. This phenomenon is similar to that in the DFB laser and VCSELs, where there is a maximum microwave power for a fixed frequency detuning [28,34]. The impact of Δf on the frequency and power of the generated microwave photonic signal is investigated under two injection ratios: a lower injection ratio ξ_{inj} = 0.1 and a higher injection ratio ξ_{inj} = 0.92, as shown in Figure 4c,d. There is no surprise that the microwave frequency increases with the increase in the frequency detuning because the main contribution of the generated microwave is the frequency beating of the redshift cavity frequency and the regenerated injection frequency. The microwave power decreases with the increase in the frequency detuning due to the decrease in nonlinear frequency mixing effect with increasing Δf [29].

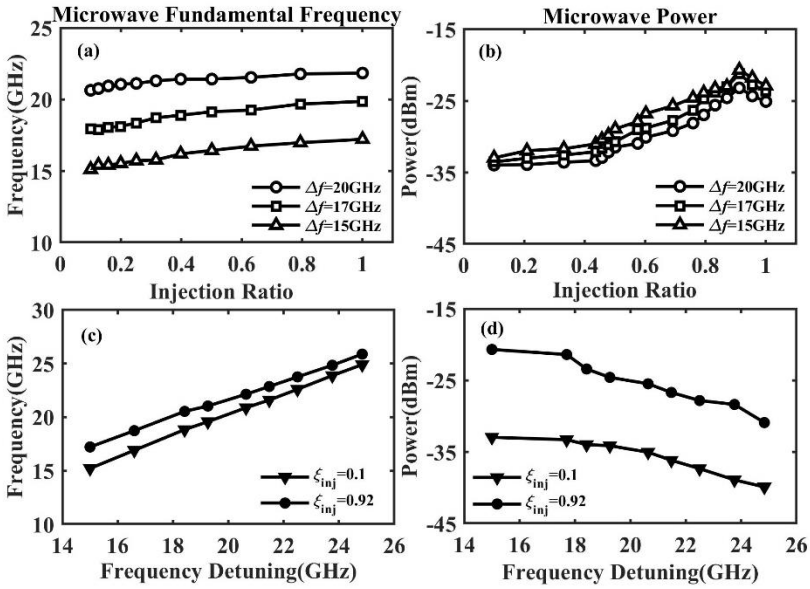

Figure 4. (**a**) Frequency and (**b**) power of the generated microwave as a function of injection ratio; (**c**) frequency and (**d**) power of the microwave versus frequency detuning.

The quality of the generated microwave in the optically injected DM laser is examined by analyzing its linewidth and phase noise. A 3 dB linewidth is adopted to quantify the linewidth, and the phase noise is obtained by integrating single sideband power spectrum

offset from 3 to 200 MHz of the fundamental frequency and then normalizing it to the microwave power. The linewidth and phase noise of the generated microwave shown in Figure 4a are calculated and displayed in Figure 5. We can see that the linewidth and phase noise of the generated microwave decrease first with the increase in ξ_{inj} until they reach their minimum values at an injection ratio ξ_{inj} of around 0.92, and upon a further increase in the injection ratio, the linewidth and phase noise of the microwave signal increase again. The minimum linewidth and phase noise of the generated microwave obtained at the injection parameters (Δf, ξ_{inj}) = (15 GHz, 0.92) are 1.8 MHz and 2.75 rad^2, respectively. The microwave linewidths produced in the optically injected DM lasers are similar to those in DFB lasers [28] but narrower than those in VCSELs [35]. This is because DM lasers have very narrow linewidths [40]. Comparing Figure 5 with Figure 4b, we can see that the linewidth and phase noise of the generated microwaves reach their local minima at the injection ratio where the maximum microwave power is achieved; these results are identical compared to those reported in DFB lasers [28].

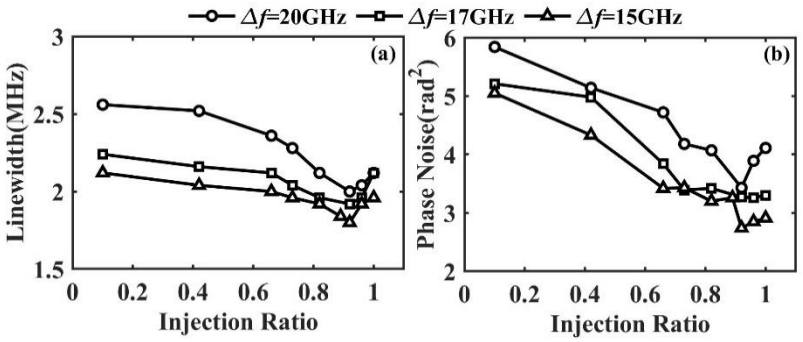

Figure 5. (**a**) Linewidth and (**b**) phase noise of the generated microwave versus ξ_{inj}.

In order to stabilize the fluctuation of the generated microwave and reduce its linewidth, the optical feedback technique used in DFB lasers and VCSELs [28,44] is adopted. In this experiment, only a single feedback loop is introduced. Figure 6 presents the power spectra of the DM laser (a) without optical feedback and (b) with optical feedback at the injection parameters of (Δf, ξ_{inj}) = (15 GHz, 0.92). At these injection parameters, the fundamental frequency of the microwave is 17.2 GHz. As shown in Figure 6a, the linewidth of the generated microwave photonic signal is 1.8 MHz without optical feedback. After introducing the optical feedback, the linewidth decreases. Figure 6b shows that the linewidth narrows from 1.82 to 0.52 MHz when the feedback ratio is −27.8 dB and the feedback round trip time is 96.15 ns. Many side peaks equally separated by multiple of 10.4 MHz also appear in Figure 6b, which corresponds to the external cavity modes' frequencies. To quantify the side peaks in the power spectrum, a concept of side peak suppression (SPS) is introduced and is defined as the ratio of the power at the fundamental frequency to the maximum power of the side peaks [43]. The SPS is around 28 dB, as shown in Figure 6b.

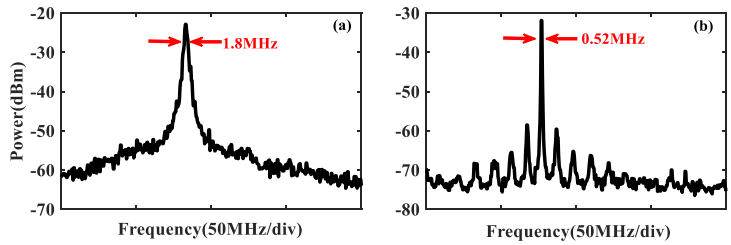

Figure 6. Power spectra of the DM laser (**a**) without and (**b**) with optical feedback. The injection parameters (Δf, ξ_{inj}) = (15 GHz, 0.92).

The effects of the optical feedback ratio on the linewidth, phase noise, and SPS of the generated microwave in the optically injected DM laser are studied and shown in

Figure 7. The parameters in Figure 7 are the same as those in Figure 6b except for the optical feedback ratio. Figure 7a shows that the linewidth first decreases as the feedback ratio increases. When the feedback ratio is increased to −35.7 dB, the linewidth remains almost constant as the feedback ratio is further increased until the feedback ratio reaches −25.7 dB. Upon a further increase in the optical feedback ratio, the linewidth increases again. This variation trend is different from that in the DFB laser and VCSEL [28,35] but is similar to that in the DFB laser with filter feedback at some frequency detuning [45]. The relationship between the phase noise and the feedback ratio is similar to that of the linewidth. As the feedback ratio increases, the phase noise first decreases, then remains constant at around 0.3 rad^2, and then increases again. Figure 7c presents SPS as a function of feedback ratio. When the feedback ratio is −42.7 dB, the SPS is 30.3 dB. The SPS starts to decrease first when the feedback strength increases, which is similar to that in the DFB laser and VCSEL [28,35]. However, after the feedback ratio increases to −35.8 dB, upon a further increase in the feedback ratio, the SPS remains almost constant at a value of about 28.3 dB until the feedback ratio reaches −25.7 dB. Beyond the aforementioned feedback ratio, the SPS decreases sharply. This is because the DM laser is about to leave the P1 dynamic. Figure 7 shows that the SPS remains above 25 dB within the feedback ratios where the linewidth and phase noise are kept to their minimum. The results indicate that a high SPS can be maintained over a wide feedback ratio range in the optically injected DM laser with a single optical feedback loop. The different variations shown in Figure 7 compared to those in DFB lasers and VCSELs may be attributed to the filtering effect caused by the structure of the DM laser, but further study is needed to fully understand the characteristics of DM lasers.

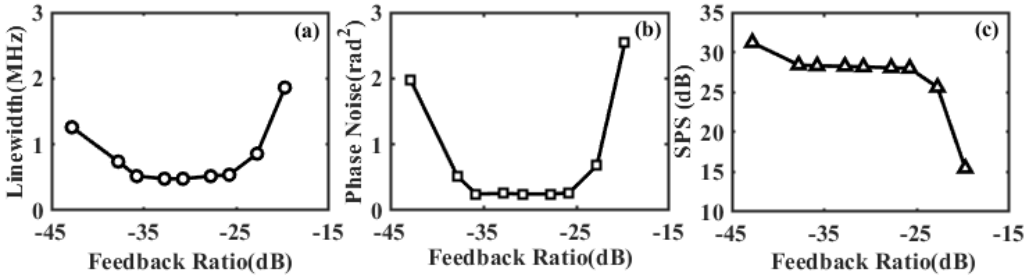

Figure 7. (**a**) Linewidth, (**b**) phase noise variance, and (**c**) side peak suppression of the generated microwave as a function of the feedback ratio. The injection parameters (Δf, ξ_{inj}) are (15 GHz, 0.92).

4. Theoretical Model and Analysis

Dynamics of the optically injected DM laser and the characteristics of the generated microwave based on the P1 dynamic in the optically injected DM laser are numerically simulated using the model in [46] and by considering the nonlinear carrier recombination [47].

$$\frac{dE(t)}{dt} = \frac{(1+i\alpha)}{2}\left[\frac{g(N-N_0)}{1+\varepsilon|E(t)|^2} - \frac{1}{\tau_p}\right]E(t) + \eta E_{inj}e^{i2\pi\Delta f t} + \kappa E(t-\tau_{ext})e^{-i\omega\tau_{ext}} \quad (1)$$

$$\frac{dN(t)}{dt} = \frac{I}{e} - \left(AN + BN^2 + CN^3\right) - \frac{g(N-N_0)|E(t)|^2}{1+\varepsilon|E(t)|^2} \quad (2)$$

where $E(t)$ is the slowly varying complex amplitude of the electric field and E_{inj} is the injection field amplitude. $N(t)$ represents the carrier number, α is the linewidth-enhanced factor, g is the differential gain coefficient, N_0 is the transparency carrier number, ε is the gain saturation factor, τ_p is the photon lifetime, τ_{ext} is the feedback round trip time of optical feedback loop, ω is the angular frequency of the laser, η denotes the injection strength, κ denotes feedback strength from the optical feedback loop, I is the injection current, e is the electron charge, A is the nonradiative modulus, B is the spontaneous modulus, and C is the Auger recombination modulus. The parameter values

used in [47] are adopted, where $\alpha = 3$, $g = 1.48 \times 10^4$ s^{-1}, $I = 30$ mA, $N_0 = 1.93 \times 10^7$, $\varepsilon = 7.73 \times 10^{-8}$, $\tau_p = 2.17$ ps, $A = 2.8 \times 10^8$ s^{-1}, $B = 9.8$ s^{-1}, and $C = 3.84 \times 10^{-7}$ s^{-1}. The relaxation oscillation frequency of the free-running laser is approximately $f_r = (gE^2/\tau_p)^{1/2}/2\pi = 6.2$ GHz. Equations (1) and (2) are solved using the second-order Runge–Kutta algorithm.

The dynamical map of the DM laser in the parameter space of frequency detuning Δf and injection strength η is presented in Figure 8a. The result is qualitatively consistent with the experimental measurements in Figure 3. To validate the model used in the simulation, we also simulated the dynamical map of the DFB laser using the model and parameters of [48], and the results are shown in Figure 8b. Figure 8b shows only one small non-P1 island within the P1 region above the Hopf bifurcation line, which is different from the experimental observation. Therefore, it is necessary to include the nonlinear carrier recombination for the investigation of the nonlinear dynamics of the optically injected DM laser.

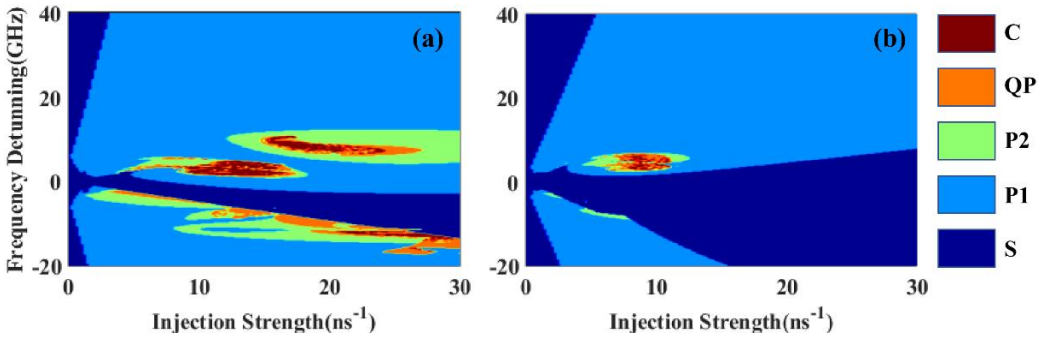

Figure 8. Numerical simulation of the dynamical maps of (**a**) the optically injected DM laser with the consideration of the nonlinear carrier recombination and (**b**) the optically injected DFB laser.

The SPS as a function of feedback strength for the generated MWP signal in the optically injected DM laser and DFB laser with single optical feedback is calculated and displayed in Figure 9. The injection parameters (Δf, η) are set at (15 GHz, 8 ns^{-1}), and the feedback round trip time is 10 ns. Figure 9 shows that for the DM laser, the SPS is ~17.1 dB at the feedback strength of 0.32 ns^{-1}. When the feedback strength is increased, the SPS starts to drop, and when the feedback strength reaches 0.4 ns^{-1}, the SPS decreases to ~14.1 dB. However, when further increasing the feedback strength, the SPS remains almost unchanged until the feedback strength reaches 0.5 ns^{-1}. When the feedback strength is increased further, the SPS starts to deteriorate again. However, for the DFB laser, the SPS decreases monotonically with the increase in the feedback strength. These results are qualitatively consistent with our experimental results in the DM laser and the reported results in the DFB laser, which indicates that single optical feedback is sufficient to achieve a narrow microwave linewidth in the optically injected DM laser.

The variations of the fundamental frequency as a function of injection strength under two frequency detunings of 15 and 20 GHz are calculated for the optically injected DM laser and optically injected DFB laser. The different variation of the fundamental frequency between the DM laser and DFB laser is illustrated in Figure 10. We can see that for the DFB laser, the fundamental frequency variation with the injection strength is similar to the report [43], where the frequency change rate for the lower injection strength is smaller compared to that for a higher injection strength. However, for the optically injected DM laser, the fundamental frequency increases linearly with the injection strength. This linear relationship implies that DM lasers may be a better candidate for frequency-modulation continuous-wave microwave generation based on the P1 dynamic.

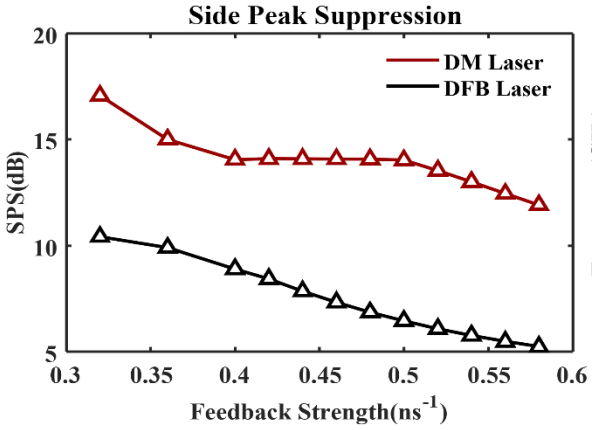

Figure 9. Numerical simulation of SPS of the generated microwave as a function of the feedback strength utilizing DM laser model and DFB laser model with the injection parameters $(\Delta f, \eta) = (15\ \text{GHz}, 8\ \text{ns}^{-1})$.

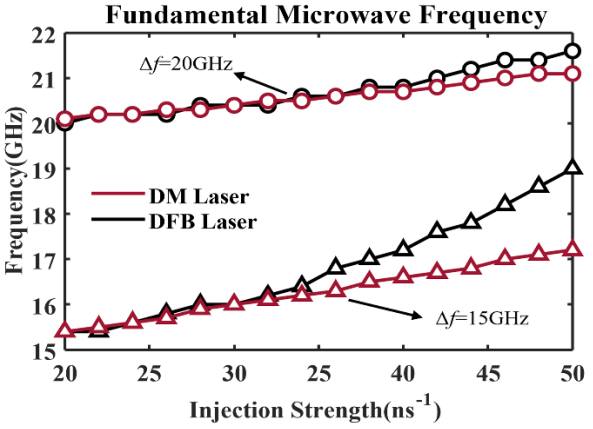

Figure 10. Numerical simulation of the generated microwave frequency as a function of the injection strength utilizing DM laser model and DFB laser model. Δf = 15 and 20 GHz.

5. Discussion

In the experiment, due to the limitation of the bandwidth of the spectrum analyzer and the maximum output power of the ML, only the injection parameters with the injection ratio ≤ 1 and the frequency detuning ≤ 26 GHz are investigated. The experimental results show that the fundamental microwave frequency increases linearly with the increase in the frequency detuning and injection ratio. It has been reported that the generated microwave frequency at a strong injection ratio still increases linearly with the injection ratio in other types of lasers [34,43]. The properties of the MWP signal generation in the DM laser at larger frequency detuning and stronger injection power will be investigated in future studies. The linewidth of the generated microwave is related to the linewidth of the ML and SL; therefore, the generated microwave linewidth in the DM laser is comparable to that in the DFB laser and narrower than that in the VCSEL. In the experiment, the microwave linewidths produced in the optically injected DM lasers with and without optical feedback are still in the range of hundreds of kilohertz to several megahertz. The linewidth of the generated microwave in the DFB laser can be reduced to a few hertz or even millihertz by optical modulation sideband injection locking or optoelectronic feedback [49,50]. Therefore, further reduction of the generated microwave linewidth in the DM laser will be undertaken in our next investigation. In addition, the relationship between the linewidth of the generated microwave and the feedback strength in an optically injected semiconductor laser subject to filtered optical feedback is related to the injection parameters [45], so it is

worth further studying the relationship between the linewidth and the feedback strength in the DM laser at other injection parameters.

6. Conclusions

In summary, we experimentally and theoretically investigated MWP signal generation based on the P1 dynamic of optically injected DM semiconductor lasers. The experimental results show that the frequency of the generated microwave can be tuned by changing the optical injection ratio or frequency detuning. The results also show that the linewidth of the generated microwave in the DM laser is comparable to that in DFB lasers and narrower compared to that in VCSELs, which may be due to the narrow linewidth of the DM laser. In addition, when introducing optical feedback, the relationship between the linewidth and the feedback ratio in the DM laser is similar to that in the DFB laser with filter feedback, which can be attributed to the filtering effect caused by the structure of the DM laser. Furthermore, an SPS of >25 dB can remain over a wide range of the feedback ratio; this suggests that single optical feedback is sufficient for reducing the linewidth of the generated microwave in the DM laser. Numerical simulations with the consideration of the nonlinear carrier recombination confirm that high SPSs can be maintained over a wide range of optical feedback strength, which is in good agreement with the results obtained in the experiment.

Author Contributions: Conceptualization, D.C., Z.Z., A.V., Y.H.; data curation, D.C., Z.Z., Y.H.; formal analysis, D.C., Z.Z., Y.H., W.J., S.J.; funding acquisition, Y.H., J.T., A.V.; investigation, D.C., Z.Z., A.V., Y.H.; methodology, D.C., Z.Z., J.T., Y.H.; project administration, Y.H., J.T., A.V.; software, D.C., Z.Z.; supervision, Z.Z., Y.H.; validation, D.C., Z.Z., Y.H.; visualization, D.C., Z.Z., Y.H.; writing—original draft, D.C., Z.Z.; writing—review and editing, D.C., Z.Z., A.V., W.J., S.J., J.T., Y.H. All authors have read and agreed to the published version of the manuscript.

Funding: This research was funded in part by the DESTINI project (2017/COL/007) funded by the ERDF under the SMART Expertise scheme; in part by the DSP Centre (82085) funded by the ERDF through the Welsh Government; and in part by Ministerio de Ciencia e Innovación, Spain, under grant RTI2018-094118-B-C22 MCIN/AEI/FEDER, UE.

Informed Consent Statement: Not applicable.

Data Availability Statement: Not applicable.

Acknowledgments: D. Chang is thankful for the support of Bangor University's Great Heritage PhD studentship.

Conflicts of Interest: The authors declare no conflict of interest.

References

1. Yao, J. Microwave Photonics. *J. Light. Technol.* **2009**, *27*, 314–335. [CrossRef]
2. Pan, S.; Zhang, Y. Microwave photonic radars. *J. Light. Technol.* **2020**, *38*, 5450–5484. [CrossRef]
3. Nie, B.; Ruan, Y.; Yu, Y.; Guo, Q.; Xi, J.; Tong, J. Period-one microwave photonic sensing by a laser diode with optical feedback. *J. Light. Technol.* **2020**, *38*, 5423–5429. [CrossRef]
4. William, J.; Shain, N.A.; Vickers, A.N.; Thomas, B.; Anne, S.; Jerome, M. Dual fluorescence-absorption deconvolution applied to extended-depth-of-field microscopy. *Opt. Lett.* **2017**, *42*, 4183–4186.
5. Xu, C.; Zhou, L.; Zhou, J.Y.; Boggs, S. High frequency properties of shielded power cable-part 1: Overview of mechanisms. *IEEE Electr. Insul. Mag.* **2005**, *21*, 24–28.
6. Carpintero, G.; Balakier, K.; Yang, Z.; Guzm'an, R.C.; Corradi, A.; Jimenez, A.; Kervella, G.; Fice, M.J.; Lamponi, M.; Chitoui, M.; et al. Microwave Photonic integrated circuits for millimeter-wave wireless communications. *J. Light. Technol.* **2014**, *32*, 3495–3501. [CrossRef]
7. Wu, J.; Peng, J.; Liu, B.; Pan, T.; Zhou, H.; Mao, J.; Yang, Y.; Qiu, C.; Su, Y. Passive silicon photonic devices for microwave photonic signal processing. *Opt. Commun.* **2016**, *373*, 44–52. [CrossRef]
8. Liu, J.; Lucas, E.; Raja, A.S.; He, J.; Riemensberger, J.; Wang, R.N.; Karpov, M.; Guo, H.; Bouchand, R.; Kippenberg, T.J. Photonic microwave generation in the X- and K-band using integrated soliton microcombs. *Nat. Photonics* **2020**, *14*, 486–491. [CrossRef]
9. Islam, M.S.; Kovalev, A.V.; Coget, G.; Viktorov, E.A.; Citrin, D.S.; Locquet, A. Staircase dynamics of a photonic microwave oscillator based on a laser diode with delayed optoelectronic feedback. *Phys. Rev. Appl.* **2020**, *13*, 064038. [CrossRef]

10. Xie, X.; Bouchand, R.; Nicolodi, D.; Giunta, M.; Hänsel, W.; Lezius, M.; Joshi, A.; Datta, S.; Alexandre, C.; Lours, M.; et al. Photonic microwave signals with zeptosecond-level absolute timing noise. *Nat. Photonics* **2017**, *11*, 44–47. [CrossRef]
11. Xue, X.; Xuan, Y.; Bao, C.; Li, S.; Zheng, X.; Zhou, B.; Qi, M.; Weiner, A.M. Microcomb-based true-time-delay network for microwave beamforming with arbitrary beam pattern control. *J. Light. Technol.* **2018**, *36*, 2312–2321. [CrossRef]
12. Bünermann, O.; Jiang, H.; Dorenkamp, Y.; Kandratsenka, A.; Janke, S.M.; Auerbach, D.J.; Wodtke, A.M. Electron-hole pair excitation determines the mechanism of hydrogen atom adsorption. *Science* **2015**, *350*, 1346–1349. [CrossRef] [PubMed]
13. Gliese, U.; Nielsen, T.N.; Bruun, M.; Christensen, E.L.; Stubkjaer, K.E.; Lindgren, S.; Broberg, B. A wideband heterodyne optical phase-locked loop for generation of 3-18 GHz microwave carriers. *IEEE Photonics Technol. Lett.* **1992**, *4*, 936–938. [CrossRef]
14. Kittlaus, E.A.; Eliyahu, D.; Ganji, S.; Williams, S.; Matsko, A.B.; Cooper, K.B.; Forouhar, S. A low-noise photonic heterodyne synthesizer and its application to millimeter-wave radar. *Nat. Commun.* **2021**, *12*, 4397. [CrossRef]
15. Hwang, S.K.; Chan, S.C.; Hsieh, S.C.; Li, C.Y. Photonic microwave generation and transmission using direct modulation of stably injection-locked semiconductor lasers. *Opt. Commun.* **2011**, *284*, 3581–3589. [CrossRef]
16. Gao, Y.; Wen, A.; Zheng, H.; Liang, D.; Lin, L. Photonic microwave waveform generation based on phase modulation and tunable dispersion. *Opt. Express* **2016**, *24*, 12524–12533. [CrossRef]
17. He, Y.; Jiang, Y.; Zi, Y.; Bai, G.; Tian, J.; Xia, Y.; Zhang, X.; Dong, R.; Luo, H. Photonic microwave waveforms generation based on two cascaded single-drive Mach-Zehnder modulators. *Opt. Express* **2018**, *26*, 7829–7841. [CrossRef]
18. Dal Bosco, A.K.; Kanno, K.; Uchida, A.; Sciamanna, M.; Harayama, T.; Yoshimura, K. Cycles of self-pulsations in a photonic integrated circuit. *Phys. Rev. E* **2015**, *92*, 062905. [CrossRef]
19. Sooudi, E.; Huyet, G.; McInerney, J.G.; Lelarge, F.; Merghem, K.; Martinez, A.; Ramdane, A.; Hegarty, S.P. Observation of harmonic-mode-locking in a mode-locked InAs/InP-based quantum-dash laser with cw optical injection. *IEEE Photonics Technol. Lett.* **2011**, *23*, 549–551. [CrossRef]
20. Zou, X.; Liu, X.; Li, W.; Li, P.; Pan, W.; Yan, L.; Shao, L. Optoelectronic oscillators (OEOs) to sensing, measurement, and detection. *IEEE J. Quantum Electron.* **2015**, *52*, 1–16. [CrossRef]
21. Liao, M.L.; Huang, Y.Z.; Weng, H.Z.; Han, J.Y.; Xiao, Z.X.; Xiao, J.L.; Yang, Y.D. Narrow-linewidth microwave generation by an optoelectronic oscillator with a directly modulated microsquare laser. *Opt. Lett.* **2017**, *42*, 4251–4254. [CrossRef] [PubMed]
22. Lin, X.D.; Wu, Z.M.; Deng, T.; Tang, X.; Fan, L.; Gao, Z.Y.; Xia, G.Q. Generation of widely tunable narrow-linewidth photonic microwave signals based on an optoelectronic oscillator using an optically injected semiconductor laser as the active tunable microwave photonic filter. *IEEE Photonics J.* **2018**, *10*, 1–9. [CrossRef]
23. Zhang, W.; Yao, J. Silicon photonic integrated optoelectronic oscillator for frequency-tunable microwave generation. *J. Light. Technol.* **2018**, *36*, 4655–4663. [CrossRef]
24. Li, M.; Hao, T.; Li, W.; Dai, Y. Tutorial on optoelectronic oscillators. *APL Photonics* **2021**, *6*, 061101. [CrossRef]
25. AlMulla, M.; Liu, J.M. Linewidth characteristics of period-one dynamics induced by optically injected semiconductor lasers. *Opt. Express* **2020**, *28*, 14677–14693. [CrossRef] [PubMed]
26. Qi, X.; Liu, J.M. Photonic microwave applications of the dynamics of semiconductor lasers. *IEEE J. Sel. Top. Quantum Electron.* **2011**, *17*, 1198–1211. [CrossRef]
27. Zhuang, J.P.; Chan, S.C. Tunable photonic microwave generation using optically injected semiconductor laser dynamics with optical feedback stabilization. *Opt. Lett.* **2013**, *38*, 344–346. [CrossRef]
28. Zhuang, J.P.; Chan, S.C. Phase noise characteristics of microwave signals generated by semiconductor laser dynamics. *Opt. Express* **2015**, *33*, 2777–2797. [CrossRef]
29. Zhang, L.; Chan, S.C. Cascaded injection of semiconductor lasers in period-one oscillations for millimeter-wave generation. *Opt. Lett.* **2019**, *44*, 4905–4908. [CrossRef]
30. Wang, C.; Raghunathan, R.; Schires, K.; Chan, S.C.; Lester, L.F.; Grillot, F. Optically injected InAs/GaAs quantum dot laser for tunable photonic microwave generation. *Opt. Lett.* **2016**, *41*, 1153–1156. [CrossRef]
31. Perez, P.; Quirce, A.; Valle, A.; Consoli, A.; Noriega, I.; Pesquera, L.; Esquivias, I. Photonic generation of microwave signals using a single-mode VCSEL subject to dual-beam orthogonal optical injection. *IEEE Photonics J.* **2015**, *7*, 1–14. [CrossRef]
32. Lin, H.; Ourari, S.; Huang, T.; Jha, A.; Briggs, A.; Bigagli, N. Photonic microwave generation in multimode VCSELs subject to orthogonal optical injection. *J. Opt. Soc. Am. B* **2017**, *34*, 2381–2389. [CrossRef]
33. Huang, Y.; Zhou, P.; Li, N. Broad tunable photonic microwave generation in an optically pumped spin-VCSEL with optical feedback stabilization. *Opt. Lett.* **2021**, *46*, 3147–3150. [CrossRef] [PubMed]
34. Ji, S.; Hong, Y.; Spencer, P.S.; Benedikt, J.; Davies, I. Broad tunable photonic microwave generation based on period-one dy-namics of optical injection vertical-cavity surface-emitting lasers. *Opt. Express* **2017**, *25*, 19863–19871. [CrossRef]
35. Ji, S.; Xue, C.P.; Valle, A.; Spencer, P.S.; Li, H.Q.; Hong, Y. Stabilization of photonic microwave generation in vertical-cavity surface-emitting lasers with optical injection and feedback. *J. Light. Technol.* **2018**, *32*, 4660–4666. [CrossRef]
36. Valle, A.; Quirce, A.; Ji, S.; Hong, Y. Polarization effects on photonic microwave generation in VCSELs under optical injection. *Photonics Technol. Lett.* **2018**, *30*, 1266–1269. [CrossRef]
37. Fan, L.; Wu, Z.M.; Deng, T.; Wu, J.G.; Tang, X.; Chen, J.J.; Mao, S.; Xia, G.Q. Subharmonic microwave modulation stabilization of tunable photonic microwave generated by period-one nonlinear dynamics of an optically injected semiconductor laser. *J. Light. Technol.* **2014**, *32*, 4660–4666. [CrossRef]

38. Ma, X.W.; Huang, Y.Z.; Zou, L.X.; Liu, B.W.; Long, H.; Weng, H.Z.; Yang, Y.D.; Xiao, J.L. Narrow-linewidth microwave generation using AlGaInAs/InP microdisk lasers subject to optical injection and optoelectronic feedback. *Opt. Express* **2015**, *23*, 20321–20331. [CrossRef]
39. Osborne, S.; O'Brien, S.; Buckley, K.; Fehse, R.; Amann, A.; Patchell, J.; Kelly, B.; Jones, D.R.; O'Gorman, J.; O'Reilly, E.P. Design of single-mode and two-color Fabry–PÉrot lasers with patterned refractive index. *IEEE J. Sel. Top. Quantum Electron.* **2007**, *13*, 1157–1163. [CrossRef]
40. Herbert, C.; Jones, D.; Kaszubowska-Anandarajah, A.; Kelly, B.; Rensing, M.; O'Carroll, J.; Phelan, R.; Anandarajah, P.; Perry, P.; Barry, L.P.; et al. Discrete mode lasers for communication applications. *IET Optoelectron.* **2009**, *3*, 1–17. [CrossRef]
41. Rosado, A.; Pérez-Serrano, A.; Tijero, J.M.G.; Gutierrez, A.V.; Pesquera, L.; Esquivias, I. Numerical and experimental analysis of optical frequency comb generation in gain-switched semiconductor lasers. *IEEE J. Quantum Electron.* **2019**, *55*, 1–12. [CrossRef]
42. Zhong, Z.; Chang, D.; Jin, W.; Lee, M.W.; Wang, A.; Jiang, S.; He, J.; Tang, J.; Hong, Y. Intermittent dynamical state switching in discrete-mode semiconductor lasers subject to optical feedback. *Photonics Res.* **2021**, *9*, 1336–1342. [CrossRef]
43. Chan, S.C.; Hwang, S.K.; Liu, J.M. Period-one oscillation for photonic microwave transmission using an optically injected semiconductor laser. *Opt. Express* **2007**, *15*, 14921–14935. [CrossRef] [PubMed]
44. Xue, C.; Chang, D.; Fan, Y.; Ji, S.; Zhang, Z.; Lin, H.; Spencer, P.S.; Hong, Y. Characteristics of microwave photonic signal generation using vertical-cavity surface-emitting lasers with optical injection and feedback. *J. Opt. Soc. Am. B* **2020**, *37*, 1394–1400. [CrossRef]
45. Xue, C.; Ji, S.; Hong, Y.; Jiang, N.; Li, H.; Qiu, K. Numerical investigation of photonic microwave generation in an optically injected semiconductor laser subject to filtered optical feedback. *Opt. Express* **2018**, *27*, 5065–5082. [CrossRef]
46. Dellunde, J.; Torrent, M.C.; Sancho, J.M.; San, M.M. Frequency dynamics of gain-switched injection-locked semiconductor lasers. *IEEE J. Quantum Electron.* **1997**, *33*, 1537–1542. [CrossRef]
47. Valle, A. Statistics of the optical phase of a gain-switched semiconductor laser for fast quantum randomness generation. *Photonics* **2021**, *8*, 388. [CrossRef]
48. Li, N.; Pan, W.; Locquet, A.; Chizhevsky, V.N.; Citrin, D.S. Statistical properties of an external-cavity semiconductor laser: Experiment and theory. *IEEE J. Sel. Top. Quantum Electron.* **2015**, *21*, 553–560.
49. Hung, Y.H.; Hwang, S.K. Photonic microwave stabilization for period-one nonlinear dynamics of semiconductor lasers using optical modulation sideband injection locking. *Opt. Express* **2015**, *23*, 6520–6532. [CrossRef]
50. Suelzer, J.S.; Simpson, T.B.; Devgan, P.; Usechak, N.G. Tunable, low-phase-noise microwave signals from an optically injected semiconductor laser with opto-electronic feedback. *Opt. Lett.* **2017**, *42*, 3181–3184. [CrossRef]